Styrene–Butadiene–Styrene/Montmorillonite Nanocomposites Synthesized by Anionic Polymerization

Zhenjun Zhang,[1,2] Lina Zhang,[1,3] Yang Li,[2] Hongde Xu[2]

[1]*Department of Chemistry, Wuhan University, Wuhan 430072, China*
[2]*Research Institute, Beijing Yanshan Petrochemical Company, Limited, Beijing 102500, China*
[3]*Center of Nanoscience and Nanotechnology, Wuhan University, Wuhan 430072, China*

Received 6 December 2004; accepted 20 April 2005
DOI 10.1002/app.22768
Published online 9 December 2005 in Wiley InterScience (www.interscience.wiley.com).

ABSTRACT: We successfully synthesized an exfoliated styrene–butadiene–styrene triblock copolymer (SBS)/montmorillonite nanocomposite by anionic polymerization. Gel permeation chromatography showed that the introduction of organophilic montmorillonite (OMMT) resulted in a small high-molecular-weight fraction of SBS in the composites, leading to a slight increase in the weight-average and number-average molecular weights as well as the polydispersity index. The results from ^{1}H-NMR revealed that the introduction of OMMT almost did not affect the microstructure of the copolymer when the OMMT concentration was lower than 4 wt %. Transmission electron microscopy and X-ray diffraction showed a completely exfoliated nanocomposite, in which both polystyrene and polybutadiene blocks entered the OMMT galleries, leading to the dispersion of OMMT layers on a nanoscale. The exfoliated nanocomposite exhibited higher thermal stability, glass-transition temperature, elongation at break, and storage modulus than pure SBS. J Appl Polym Sci 99: 2273–2278, 2006

Key words: anionic polymerization; nanocomposites; structure

INTRODUCTION

Inorganic fillers have often been used to reinforce polymers to obtain high heat durability and mechanical strength. However, as a result of the poor dispersion of inorganic fillers in the polymer matrix, conventional filled polymer composites are phase-separated macrocomposites, in which inorganic fillers have poor bonding with the matrix and only filler concentrations greater than 30% can lead to an optimum reinforcement for thermoplastics, resulting in bad processability.[1,2] Layer silicates, because of their intrinsically anisotropic character and swelling capability, have attracted much attention in the field of polymer materials. The crystal structure of a layered silicates such as montmorillonite (MMT) consists of two-dimensional layers obtained by the combination of two tetrahedral silica layers with Mg or Al to form an octahedral metal oxide. The layer thickness is about 1 nm, and the layers range from 30 nm to several micrometers. Isomorphic substitution within the layers generates negative charges that are normally counterbalanced by cations (Na^+, K^+, Ca^{2+}, …) in the galleries.[3,4] The metal cations can be exchanged with organic quaternary alkylammonium salts with long chains. The organic cations can reduce the surface energy of silicate layers and enhance the miscibility between the silicate layers and the polymer matrix, and so the distance between the layers is enlarged.[5,6] The resulting structure allows clay to accommodate polymer chains and form polymer/clay nanocomposites. Therefore, the nanocomposites possess unique properties that are not shared by conventional composites, such as excellent mechanical properties, high thermal stability, and enhanced barrier properties. In the past several years, many polymer/clay nanocomposites, such as polystyrene (PS)/clay,[7–11] rubber/clay,[12,13] polyurethane/clay,[14–16] poly(ethylene oxide)/clay,[17,18] epoxy/clay,[19–21] poly(methyl methacrylate),[22] polyamide/clay,[23] polyethylene/clay,[24] polypropylene/clay,[25] polyaniline/clay,[26,27] and poly(lactic acid)/clay,[28,29] have been found to show good properties.

The styrene–butadiene–styrene triblock copolymer (SBS) has been widely used as a thermoplastic elastomer. Laus et al.[30] for the first time prepared intercalated SBS/clay nanocomposites by melt blending, and the nanocomposites exhibited enhanced moduli. Chen and Gong[31] prepared SBS/clay nanocomposites through direct melt intercalation and indicated a new glass-transition temperature around 157°C for the nanocomposites. Liao et al.[32] reported an intercalated SBS/clay nanocomposite by a solution approach, in-

Correspondence to: L. Zhang (lnzhang@public.wh.hb.cn).
Contract grant sponsor: Center of Nanomaterials of Wuhan University.
Contract grant sponsor: Institute of Chemistry of the Chinese Academy of Sciences.

dicating that the nanocomposites exhibited increased thermal and mechanical properties. Recently, Zhang et al.[33] prepared intercalated SBS/clay nanocomposites, which showed improved radiation stability in comparison with pure SBS. However, completely exfoliated SBS/clay nanocomposites have scarcely been reported. With exfoliation, the physical properties of the nanocomposites can be obviously improved because of the occurrence of a large polymer/filler interface.[34,35]

Living polymerization provides the best methodology for the synthesis of polymers with predictable molecular weights and nearly monodisperse distributions of the molecular weight.[36] Therefore, we are interested in the structure and properties of highly exfoliated SBS/clay nanocomposites prepared by living anionic polymerization. In our previous work, a new fabrication of styrene–butadiene rubber/MMT nanocomposites by anionic polymerization was studied, and an improvement in the mechanical properties and thermal stability was indicated.[37] In this study, exfoliated SBS/MMT nanocomposites were synthesized by anionic polymerization with *n*-butyllithium (*n*-BuLi) as an initiator. The effect of the organophilic montmorillonite (OMMT) content on the structure and properties of the nanocomposites was investigated and discussed.

EXPERIMENTAL

Materials

OMMT (Nannolin DK4) was supplied by Fenghong Clay Chemical Corp. (Zheijiang, China). The clay was exchanged by a quaternary long organic ammonium salt with a cation-exchange capacity of 110 mequiv/100 g to obtain an average particle size of 25 μm in the dry state. All materials used were purified as follows before use. Styrene (St; Yanshan Petrochemical Co., Beijing,
China; polymerization-grade) was treated with activate alumina to remove the inhibitor and deoxygenated. Butadiene (Bd; Yanshan Petrochemical; polymerization-grade) was treated with minor *n*-BuLi to remove the moisture and inhibitor. Cyclohexane (Jinxi Chemical Plant, Beijing, China; chemical-grade) was dried with 5-Å molecular sieves and deoxygenated. *n*-BuLi was self-made, and its concentration was calibrated by the Gilman double-titration method.[38] Tetrahydrofuran (THF; Beijing Yili Fineness Chemical Factory, Beijing, China) was analytical-grade and was refluxed over CaH_2 for more than 4 h and then distilled.

Synthesis of the SBS/MMT nanocomposites

Given amounts of St, THF (THF/*n*-BuLi = 2), OMMT, and cyclohexane were introduced into a 5-L polymerization kettle filled with purified N_2. After 3 h of stirring, a little *n*-BuLi was added to remove impurities in the system, and then a stoichiometric amount (according to a designed molecular weight of 9×10^4) of *n*-BuLi as an initiator was added to the kettle. The polymerization was carried out at 50°C for 2 h. Then, Bd was added to the kettle to continue the polymerization, which formed poly(styrene-*b*-butadiene) diblock anions. After 2.5 h, the same amount of the beginning St was added. Two hours later, a small amount of absolute ethyl alcohol was added to terminate the living styryl lithium chains. The product (St/Bd = 42:58) was vacuum-dried at 80°C for 24 h. The pure SBS sample and SBS/MMT nanocomposites, which contained 1, 2, 3, and 4 wt % OMMT, were coded as SBS, SBS-M1, SBS-M2, SBS-M3, and SBS-M4, respectively. For the SBS-M3 sample, before Bd was introduced, a little of the polymerization solution was taken out and terminated, and the resulting product was coded PS-M3.

Characterization

The molecular weights and molecular weight distributions of the polymers were measured with a gel permeation chromatograph (model 10A, Shimadzu, Kyoto, Japan) equipped with three TSKgel multipore HXL-M columns (7.8 mm $\times$ 300 cm) at room temperature. The eluent was THF. The samples were dissolved in THF overnight to prepare solutions with a 1.0 mg/mL concentration. The THF and polymer solutions were filtered with a 0.45-μm filter to remove clays and were degassed before use. The injection volume was 100 μL for each sample, and the flow rate was 1.0 mL/min. The calibration curves for gel permeation chromatography (GPC) were obtained with TSK standard samples of PS (Soda Co., Tokyo, Japan). Class LC10 software was used for the data acquisition and analysis.

X-ray diffraction (XRD) measurements of the samples were carried out with an X-ray diffractometer (D/max-II, Rigaku, Tokyo, Japan) with a Cu Kα target at 40 kV and 100 mA [wavelength (λ) = 0.154 nm] with a 2θ scan range of 2–15° (where θ is the diffraction angle). Transmission electron microscopy (TEM) analysis was carried out on a TECNAI $G^2$20 transmission electron microscope (FEI Co., Hillsboro, OR) at an acceleration voltage of 200 kV. Ultrathin sections of the samples were prepared at −120°C with a Leica Ultracut UCT (Vienna, Austria) with an EMFCS cryoattachment. Cross sections with a thickness of 50 nm were obtained with a diamond knife. To observe the morphology, the cross sections were exposed to osmium tetroxide vapor for 1 h at room temperature to selectively stain the polybutadiene (PB) phase. The ^{1}H-NMR spectrum was recorded on a DRX 400 NMR spectrometer (Bruker, Fällanden, Switzerland) at 400

TABLE I
M_n, M_w, d, and the Microstructure Values of the SBS and SBS/MMT Nanocomposites

Sample	$M_n \times 10^{-4}$	$M_w \times 10^{-4}$	d	$St_{nonblock}$	St_{block}	1,2-PB	*trans*-1,4	*cis*-1,4
SBS	8.6	9.6	1.12	1.5	43.4	8.2	30.2	18.1
SBS-M1	8.6	10.4	1.22	0.4	42.9	8.0	31.0	18.0
SBS-M2	9.3	10.9	1.17	0.4	44.9	7.7	29.4	18.0
SBS-M3	9.9	11.8	1.19	0.3	43.6	7.8	29.9	18.7
SBS-M4	12.3	15.1	1.23	2.5	39.7	8.3	32.2	19.7

MHz at 25°C. The spinning speed, pulse delay, and total numbers of scans were 20 Hz, 15 s, and 128, respectively. The sample was dissolved in deuterated chloroform to prepare the polymer solution concentration of 150 mg/mL.

Thermogravimetric analysis measurements were performed with a TGA 2050 thermogravimetric analyzer (TA, New Castle, DE). The samples were heated to 600°C at a heating rate of 20°C/min under a nitrogen atmosphere. Dynamic mechanical analysis (DMA) was carried out with a DMA-2980 dynamic mechanical analyzer (TA) at a heating rate of 3 K/min from −130 to 200°C. The vibration frequency was 1 Hz. The specimens were about 1.5 × 4.5 × 20 mm. The mechanical properties of the sheets were measured with an electron tensile tester (AG-20KNG, Shimadzu, Kyoto, Japan) at a tensile rate of 500 mm/min according to the standard method (GB/T 528, China). The reported values are averages of five measurements.

RESULTS AND DISCUSSION

Effect of OMMT on copolymerization

GPC chromatograms of the SBS and SBS/MMT samples were obtained (not shown), and the number-average molecular weight (M_n), the weight-average molecular weight (M_w), and polydispersity index (d) are summarized in Table I. The values of M_n, M_w, and d of the SBS/MMT nanocomposites increased slightly with an increase in the OMMT content. It is well known that M_w is highly sensitive to the presence of a small amount by weight of a high-molecular weight fraction, whereas M_n is sensitive to the presence of a small fraction of low molecular weight. This indicates the absence of a low-molecular-weight fraction caused by the obvious termination of the living chains in this case. The results reveal that the introduction of OMMT caused an increase in high-molecular-weight macromolecules. This can be attributed to the fact that OMMT affected in some way the living chains by combination or transference and physical crosslinking between the SBS chains, and a small fraction of nanoparticles of OMMT remained as a junction in the solution, leading to the occurrence of small amounts of high-molecular-weight macromolecules. On the basis of the results from GPC, the addition of OMMT did not affect the living copolymerization on the whole.

The ^{1}H-NMR spectra of SBS, SBS-M1, and SBS-M3 are shown in Figure 1. The resonance peak of the ortho proton (H_o) appears at 6.58 ppm and is assigned to the characteristic of the block St. Two peaks around $\delta = 5.0$ and 5.4 ppm were derived from protons of the double bonds of 1,2- and 1,4-Bd units, and a peak at $\delta = 1.5$ is assigned to methylene in Bd units. With the addition of OMMT, almost none of the peaks changed. The contents of 1,2-polybutadiene (1,2-PB), *trans*-1,4-polybutadiene (*trans*-1,4), *cis*-1,4-polybutadiene (*cis*-1,4), block styrene (St_{block}) and nonblock styrene ($St_{nonblock}$) were analyzed according to the literature,[39] and the results are listed in Table I. The calculated proportion of monomers in the polymers was in accord with the actually added monomer ratio. The percentages of 1,2-PB, *trans*-1,4, and *cis*-1,4 of the nanocomposites hardly changed in comparison with that of SBS. This further indicated that a small addition of OMMT hardly changed the copolymerization and microstructure of the copolymer.

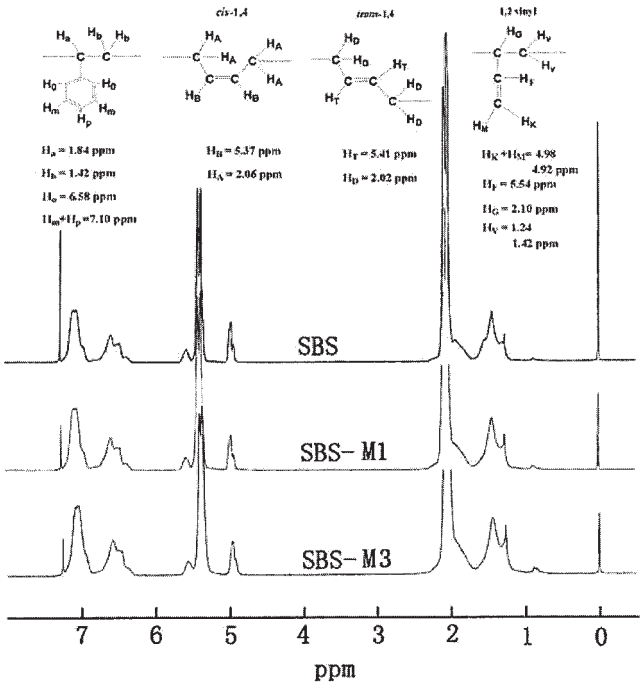

Figure 1 ^{1}H-NMR spectra of SBS, SBS-M1, and SBS-M3.

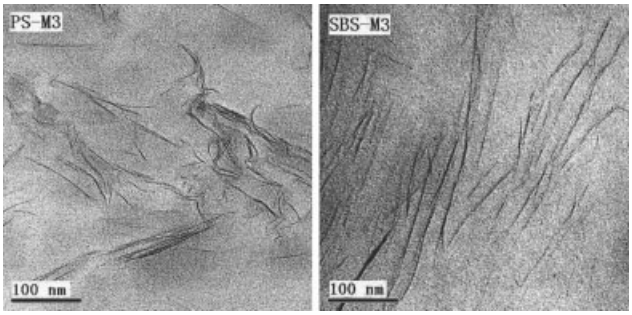

Figure 2 TEM images of PS-M3 and SBS-M3.

Structure of SBS/MMT

Figure 2 shows TEM images of PS-M3 and SBS-M3. The dark lines correspond to silicate layers. There were no large clay tactoids, and this suggested a good dispersion of OMMT in the SBS matrix. However, there were some intercalated structures in PS-M3, and this indicated that the OMMT layers were not completely exfoliated in the polymer before Bd was introduced. After the introduction of Bd and St, a completely exfoliated structure was observed, as shown in the image of SBS-M3 in Figure 2; the exfoliated OMMT layers dispersed uniformly as monolayers in the polymer matrix. The distance between the adjacent layers was in the range of 10–25 nm. The results suggest that the galleries of OMMT were further expanded after the polymerization of Bd, and this led to a highly exfoliated SBS/MMT nanocomposite.

To further investigate the morphology of the nanocomposites, TEM images of stained SBS and SBS-M3 were taken, and the images are shown in Figure 3. The dark lines and dark and light gray microdomains correspond to OMMT layers and PB and PS blocks, respectively. The image of SBS exhibits a typical microphase-separated structure because of the thermodynamic incompatibility [solubility parameters δ_{PS} = 9.1 (cal/cm$^{3)1/2}$ and δ_{PB} = 8.4 (cal/cm$^{3)1/2}$].[40] Interestingly, both PS and PB blocks appeared in OMMT galleries. The distance between the adjacent layers was large enough to accommodate the copolymer molecules. However, with the introduction of OMMT,

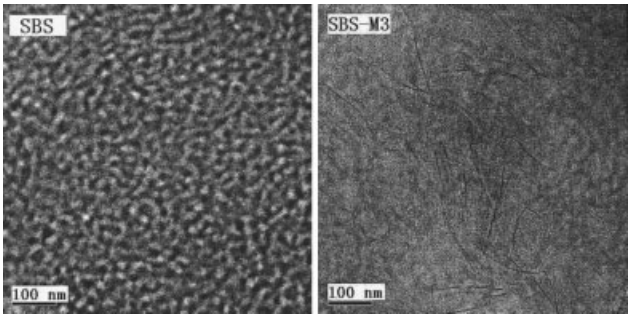

Figure 3 TEM images of stained SBS and SBS-M3.

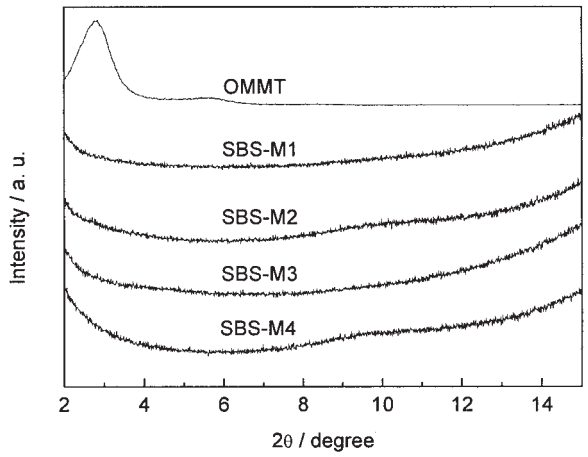

Figure 4 XRD patterns of pure OMMT and SBS/MMT nanocomposites with different OMMT contents.

the microdomains of PB and PS were not as clear as those of pure SBS, and this suggested that the interaction between the copolymer chains and OMMT layers increased the compatibility of the PS and PB blocks.

The XRD diffraction patterns of pure OMMT and SBS/MMT nanocomposites are shown in Figure 4. The d_{001} spacings [i.e., the interplanar distances of the (001) reflection plane] were calculated on the basis of Bragg's law [$d_{001} = \lambda/(2 \sin \theta)$] at the peak position. The diffraction pattern of the (001) plane of OMMT occurred at 2.46°, and the corresponding distance between the adjacent layers was 3.59 nm. There was no characteristic peak of MMT in the XRD patterns for the sheets of the SBS/MMT nanocomposites. This result further confirmed that the OMMT layers were exfoliated, and this led to the destruction of the MMT crystallite as a result of the strong interaction between OMMT and the copolymer.

Effect of the OMMT content on the properties

Derivative thermogravimetry (DTG) curves of SBS and SBS/MMT nanocomposites are shown in Figure

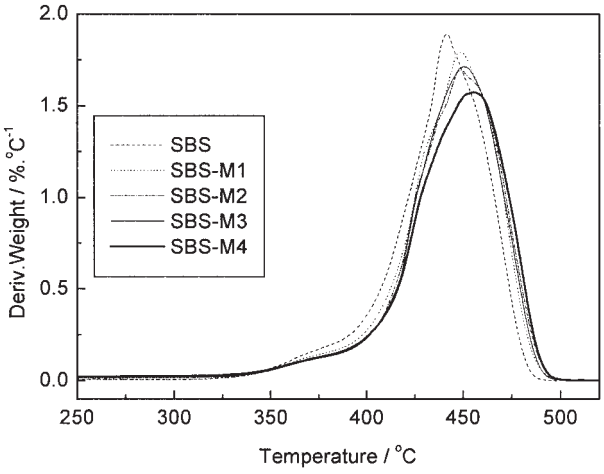

Figure 5 DTG curves of SBS and SBS/MMT nanocomposites.

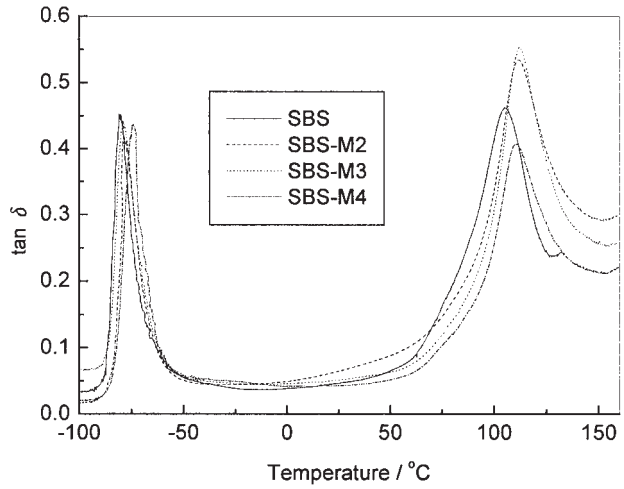

Figure 6 Temperature dependence of tan δ for SBS and SBS/MMT nanocomposites.

5. The peak temperature represents the fastest decomposition temperature. The peak of the pure SBS sample appears at 441.2°C. With an increase in OMMT, the peaks of the nanocomposites all shifted to high temperatures. Increases in the decomposition temperature of 10.2 and 14.1°C can be observed for SBS-M3 and SBS-M4, respectively, indicating an increase in the thermal stability. Therefore, the nanocomposites possessed higher thermal stability than SBS because of the strong interaction between exfoliated OMMT layers and SBS.

The DMA curves of SBS and SBS/MMT nanocomposites are shown in Figures 6 and 7, and the corresponding data are summarized in Table II. The storage modulus (E') in the plateau region between the two glass transition increased obviously with an increase in OMMT until 4 wt %, and this indicated an increase

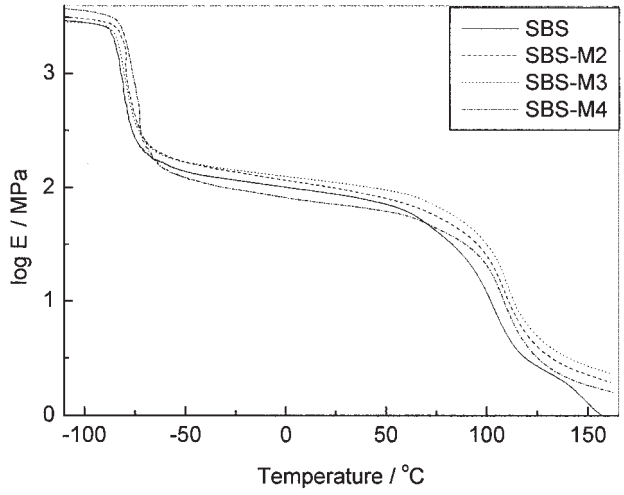

Figure 7 Temperature dependence of E' for SBS and SBS/MMT nanocomposites.

TABLE II
Thermal Data from DMA and the Mechanical Properties of the SBS and SBS/MMT Nanocomposites

Sample	T_{g1} (°C)	T_{g2} (°C)	σ_b (MPa)	ε_b (%)
SBS	−80.3	105.5	27.3	680
SBS-M1	—	—	22.4	700
SBS-M2	−78.3	111.9	22.5	740
SBS-M3	−79.3	112.3	19.8	770
SBS-M4	−73.9	110.7	10.1	730

in stiffness for the nanocomposites. In comparison with SBS, an increment of 27% in E' was observed for SBS-M3. However, with a greater increase in OMMT, such as for SBS-M4, E' decreased because excessive OMMT resulted in phase separation. The α-relaxation peak is related to the glass transition and may be analyzed to provide qualitative insight into the inner structure of a material.[41] There were two obvious α-relaxation peaks around −80 and 105°C in the tan δ curves, which were assigned to the glass-transition temperatures of the PB (T_{g1}) and PS blocks (T_{g2}), respectively. With an increase in OMMT, the tan δ peaks of both PB and PS for the nanocomposites shifted toward high temperatures. The results from DMA indicated that both PB and PS blocks intercalated into the silicate galleries because of their strong interaction.

The mechanical properties of the composites are listed in Table II. The tensile strengths (σ_b) of the nanocomposites were somewhat lower, whereas the elongations at break (ε_b) of the nanocomposites were higher, than those of SBS. This can be explained as follows: the strong interaction between the OMMT layers and copolymer chains resulted in physical crosslinking networks and a relative increase in the free volume between the copolymers, leading to the decrease in σ_b and the increase in ε_b of the nanocomposites.

CONCLUSIONS

SBS/MMT nanocomposites were synthesized successfully from St, Bd, and OMMT with an anionic method. A small addition of OMMT hardly changed the living copolymerization and microstructure of the SBS nanocomposites. However, the introduction of OMMT resulted an increase in the molecular weight of SBS in the nanocomposites, in comparison with pure SBS, and this indicated the presence of small amounts of high-molecular-weight macromolecules. The highly exfoliated structure of the SBS/MMT nanocomposites was confirmed by TEM and XRD, which showed that OMMT layers were dispersed on a nanoscale in the SBS matrix. Strong interactions existed between OMMT and SBS, leading to an improvement in the

thermal stability, glass-transition temperature, and E' in comparison with those of SBS.

References

1. Chen, T. K.; Tien, Y. I.; Wei, K. H. J Polym Sci Part A: Polym Chem 1999, 37, 2225.
2. Tjong, S. C.; Meng, T. Z.; Hay, A. S. Chem Mater 2002, 14, 44.
3. Giannelis, E. P. Adv Mater 1996, 8, 29.
4. Manchado, L. M.; Herrero, B.; Arroyo, M. Polym Int 2003, 52, 1070.
5. Mousa, A.; Karger-Kocsis, J. Macromol Mater Eng 2001, 286, 260.
6. Tien, Y. I.; Wei, K. H. Polymer 2001, 42, 3213.
7. Vaia, R. A.; Ishii, H.; Giannelis, E. P. Chem Mater 1993, 5, 1694.
8. Akelah, A.; Moet, A. Mater Lett 1993, 18, 97.
9. Fu, X.; Qutubuddin, S. Polymer 2001, 42, 807.
10. Kim, T. H.; Jang, L. W.; Lee, D. C.; Choi, H. J.; Jhon, M. S. Macromol Rapid Commun 2002, 23, 191.
11. Kim, Y. K.; Choi, Y. S.; Wang, K. H.; Chung, I. J. Chem Mater 2002, 14, 4990.
12. Joly, S.; Garnaud, G.; Ollitrault, R.; Bokobza, L. Chem Mater 2002, 14, 4202.
13. Hasegawa, N.; Okamoto, H.; Usuki, A. J Appl Polym Sci 2004, 93, 758.
14. Zilg, C.; Thomann, R.; Mülhaupt, R.; Finter, J. Adv Mater 1999, 11, 49.
15. Ni, P.; Li, J.; Suo, J.; Li, S. J Appl Polym Sci 2004, 94, 534.
16. Chen, T.; Tien, Y.; Wei, K. Polymer 2000, 42, 1345.
17. Bujdak, J.; Hackett, E.; Giannelis, E. P. Chem Mater 2000, 12, 2168.
18. Malwitz, M. M.; Dundigalla, A.; Ferreiro, V.; Butler, P. D.; Henk, M. C.; Schmidt, G. Phys Chem Chem Phys 2004, 6, 2977.
19. Zerda, A. S.; Lesser, A. J. J Polym Sci Part B: Polym Phys 2001, 39, 1137.
20. Kornmann, X.; Lindberg, H.; Berglund, L. A. Polymer 2001, 42, 1303.
21. Liu, T.; Tjiu, W. C.; Tong, Y.; He, C.; Goh, S. S.; Chung, T. J Appl Polym Sci 2004, 94, 1236.
22. Yeh, J.; Liou, S.; Lai, M.; Chang, Y.; Huang, C.; Chen, C.; Jaw, J.; Tsai, T.; Yu, Y. J Appl Polym Sci 2004, 94, 1936.
23. Liu, X.; Wu, Q.; Berglund, L. A.; Fan, J.; Qi, Z. Polymer 2001, 42, 8235.
24. Song, L.; Hu, Y.; Wang, S.; Chen, Z.; Fan, W. J Mater Chem 2002, 12, 3152.
25. Tjong, S. C.; Meng, Y. Z.; Hay, A. S. Chem Mater 2002, 14, 44.
26. Lu, J.; Zhao, X. J Mater Chem 2002, 12, 2603.
27. Lee, D.; Char, K.; Lee, S. W.; Park, Y. W. J Mater Chem 2003, 13, 2942.
28. Chang, J. H.; An, Y. U.; Cho, D.; Giannelis, E. P. Polymer 2003, 44, 3715.
29. Nam, P. H.; Fujimori, A.; Masuko, T. J Appl Polym Sci 2004, 93, 2711.
30. Laus, M.; Francescangeli, O.; Sandrolini, F. J Mater Res 1997, 12, 3134.
31. Chen, Z.; Gong, K. J Appl Polym Sci 2002, 84, 1499.
32. Liao, M.; Zhu, J.; Xu, H.; Li, Y.; Shan, W. J Appl Polym Sci 2004, 92, 3430.
33. Zhang, W.; Zeng, J.; Liu, L.; Fang, Y. J Mater Chem 2004, 14, 209.
34. Lan, T.; Kaviratna, P. D.; Pinnavaia, T. J. Chem Mater 1995, 7, 2144.
35. Yoon, J. T.; Jo, W. H.; Lee, M. S.; Ko, M. B. Polymer 2001, 42, 329.
36. Inoue, S.; Aida, T.; Kroschwitz, J. I. Encyclopedia of Polymer Science and Engineering; Wiley: New York, 1987; p 412.
37. Zhang, Z.; Zhang, L.; Li, Y.; Xu, H. Polymer 2005, 46, 129.
38. Gilman, H.; Haubein, A. H. J Am Chem Soc 1944, 66, 1515.
39. Sardelist, K.; Michels, H. J.; Allen, G. Polymer 1984, 25, 1011.
40. Grulke, E. A. In Polymer Handbook, 3rd ed.; Brandrup, J.; Immergut, H., Eds.; Wiley: New York, 1989.
41. Ishida, H.; Allen, D. J. Polymer 1996, 37, 4487.